

**Cloning and Expression of Thermophilic, Mesophilic, and Psychrophilic
Zn²⁺ Transporting ATPases**

by

Eric R. Sands

A Thesis

Submitted to the Faculty of the

WORCESTER POLYTECHNIC INSTITUTE

in partial fulfillment of the requirements for the

Degree of Master of Science

In Biochemistry

May, 2006

APPROVED:

Dr. José Argüello, Major Advisor

Dr. James Pavlik, Head of Department

TABLE OF CONTENTS

TABLE OF CONTENTS	2
ABSTRACT	3
ACKNOWLEDGEMENTS	4
LIST OF FIGURES AND TABLES	5
1.0 INTRODUCTION	6
1.1. P-type ATPases	6
1.2. P _{1B} - ATPases and Metal Specificity	7
1.3. Metal -Transport Mechanism	11
1.4. Lipids and Membrane Protein Stability	12
1.5. Project Overview	13
2.0 MATERIALS AND METHODS	15
2.1. Cloning and Protein Expression	15
2.2. Protein Purification	16
2.3. ATPase Activity Assays	17
2.4. <i>Thermotoga maritima</i> growth	18
2.5. <i>Archaeoglobus fulgidus</i> growth	18
2.6. Lipid extraction and Thin Layer Chromatography	19
3.0 RESULTS	21
3.1. <i>Escherichia coli</i> , <i>Pyrococcus abyssi</i> , and <i>Exiguobacterium 255-15</i> : Sequence homology	21
3.2. Cloning of Zn-ATPases into pBAD TOPO and pCRT7/NT	21
3.3. Expression of <i>E. coli</i> , <i>P. abyssi</i> , and <i>Exiguobacterium 255-15</i> Zn-ATPases	24
3.4. Purification of <i>E. coli</i> , <i>P. abyssi</i> , and <i>Exiguobacterium 255-15</i> Zn-ATPases	25
3.5. ATPase activity	27
3.6. Archaea Growth and TLC analysis	28
4.0 DISCUSSION	30
5.0 REFERENCES	32
Appendix	35

ABSTRACT

Protein folding and stability are essential for protein function. Changes in these characteristics can lead to altered physiological states and to the development of certain pathologies. While extensive research has focused on the stability of soluble proteins, membrane protein stability has received much less attention. Understanding the stability of membrane proteins can provide insight into folding mechanisms and the etiology of various pathologies. The purpose of this project is to prepare molecular tools to perform comparative studies of homologous membrane proteins that are found in various environments. To this end, thermophilic (*Pyrococcus abyssi*), mesophilic (*Escherichia coli*), and psychrophilic (*Exiguobacterium 255-15*) transmembrane Zn²⁺ transporting ATPases were cloned, expressed, and functionally characterized to correlate thermostability with optimal functional temperatures. In addition, the lipid environments and composition (rigid or fluid lipids) may also be involved in determining the stability of membrane proteins. Toward exploring the role of extremophilic lipids, *Archaeoglobus fulgidus* and *Thermotoga maritima* were grown and lipids were extracted. Availability of these molecular tools will enable physical-chemical studies toward understanding the structural factors that determine functional stability.

ACKNOWLEDGEMENTS

First and foremost, I want to thank Dr. José Argüello for all he has done for me in the past two years here at WPI. He has taught me so many things that I will carry forth into my career, as well as never giving up on me when things got difficult.

I also want to thank Dr. Kris Wobbe for always being helpful in providing good advice for my work in the lab.

Thank you to all of my fellow GH06 buddies: Majo, Elif, Atin, Diego, Danielle, Brad, Jyoti, Patrick, and Mike. I was very fortunate to get so many good friends in the lab, and we had lots of fun times.

I want to thank Prof. Madeline Vargas for her generosity in allowing me to perform a large amount of my research in her lab at Holy Cross

Thank you to my family and friends for not letting me give up when the times got tough.

LIST OF FIGURES AND TABLES

Figure 1: Phylogenic tree of P-type ATPases	7
Figure 2: General Topology of P _{1B} -ATPase	10
Figure 3: Scheme of P _{1B} -ATPase catalytic cycle	11
Figure 4: Sequence alignments of each Zn-ATPase	21
Figure 5: PCR amplification of <i>E. coli</i> , <i>P. abyssi</i> , and <i>Exiguobacterium 255-15</i> Zn-ATPases	22
Figure 6: PCR screening for insert orientation in <i>E. coli</i> , <i>P. abyssi</i> , and <i>Exiguobacterium 255-15</i> Zn-ATPases	23
Figure 7: Cloning maps and restriction digests	24
Figure 8: Expression of <i>E. coli</i> , <i>P. abyssi</i> , and <i>Exiguobacterium 255-15</i> Zn-ATPases using His ₆ -tagged expression vectors	25
Figure 9: Purification of <i>E. Coli</i> , <i>P. abyssi</i> , and <i>Exiguobacterium 255-15</i> Zn-ATPases	27
Figure 10: TLC plates of lipid extracts from <i>E. coli</i> , <i>Thermotoga maritima</i> , and <i>Archaeoglobus fulgidus</i>	29
Table 1: Structural characteristics of each subgroup in the P _{1B} -ATPase subfamily	9
Table 2: Clone constructs created	23
Table 3: Purification Yields	26
Table 4: ATPase Activity Yields	28

1.0 Introduction

1.1 P-type ATPases

P-type ATPases are transmembrane ion pumps that transport a variety of cations across cell membranes. These proteins are structurally characterized by six to ten transmembrane fragments (TM1-TM10), and are referred to as “P-type” because of a phosphorylated intermediate that is part of their catalytic cycle (1,2,3,5). In the catalytic cycle the energy from ATP hydrolysis is put into an electrochemical ion gradient. The cations transported may include H^+ , Na^+ , K^+ , Ca^{2+} , Cu^{2+} , Cu^+ , Cd^{2+} , Zn^{2+} and Mg^{2+} (1, 2, 5).

P-type ATPases can be further classified depending on the ions they transport across the cell membrane. There are five groups of P-type ATPases with wide phylogenetic distribution, ranging from archaea to humans (Figure 1). The P_I group is made up of: a) bacterial K^+ -ATPases and b) heavy metal (Cu^+ , Ag^+ , Cu^{2+} , Cd^{2+} , Zn^{2+} , Pb^{2+} , Co^{2+}) transporters. The P_{II} group includes: plasma membrane Ca^{2+} -ATPases, sarcoplasmic reticulum (SR) Ca^{2+} -ATPases, Na^+/K^+ , and H^+/K^+ -ATPases. The P_{III} subfamily contains H^+ and Mg^{2+} transporters. Group P_{IV} is involved with lipid transport and P_V is a group with unknown substrate specificity.



Figure 1: Phylogenetic tree of P-type ATPases (www.patbase.kvl.dk)

1.2 P_{1B}- ATPases and Metal Specificity

Heavy metals such as Cd²⁺ and Pb²⁺ can pose as a serious toxic danger to most organisms. Other metals such as Cu²⁺ and Zn²⁺ are essential nutrients required for survival (7,13). Organisms have developed sophisticated mechanisms to maintain micronutrient metal homeostasis. The heavy metal transporting ATPase membrane proteins (P_{1B} subfamily) play a vital role in regulating the efflux of these reactive elements out of various cells. Although the members of this subfamily contain similar consensus sequences, their selectivity for metals varies. As a result, sequence homology

and similarity to previously characterized P_{1B}-ATPases has divided these proteins into six groups, IB1-6 (Table 1) (1).

Proteins belonging to subgroup IB-1 transport monovalent ions such as Cu⁺ and Ag⁺. This subgroup of proteins is known for its conserved sequence NX(6)Y₁NX(4)PX(5,25)PX(6)MXXSSX(5)N/S within H7 and H8 (1). This is found in the human Menkes and Wilson disease proteins (18,19,21), *A. thaliana* HMA6 and HMA7, *E. coli* CopA (23), the yeast Cu⁺-ATPase CCC2 (22) and *A. fulgidus* CopA (6). The IB-2 proteins are found in archaea, prokaryotes, and plants, which also are characterized by their own signature sequence within H7 and H8: NX(7)KX(10,20)DXGX(7)N (1). These transporters are involved with the efflux of divalent ions such as Zn²⁺, Cd²⁺, and Pb²⁺. The first protein in the group to be functionally characterized in eukaryotic organisms was HMA2 (5). Proteins belonging to this subgroup include *E. coli* ZntA (23,25) and *H. pylori* CadA. Proteins belonging to subgroup IB-3 are found solely in prokaryotes and they transport Cu²⁺, Cu⁺ and Ag⁺. This subgroup is characterized by the sequence NX(5)GYNX(4)PX(10,20)PX(6)MSXSTX(5)N in the last two α -helices. The sequence can be found in CopB from *A. fulgidus* (11) and CopB from *E. hirae* (9). This conserved sequence from subgroup IB-3 is similar to that of IB-1 so it is no surprise that the protein is activated by Cu⁺ and Ag⁺. Subgroup IB-4 is a bit different because it contains enzymes with a total of six transmembrane fragments rather than eight. Metal selectivity was determined for CoaT from *Synechocystis* PCC6803. Studies showed that by disturbing the CoaT gene, Co²⁺ sensitivity and accumulation increases, indicating a role in Co²⁺ transport (24). Another protein belonging to this group is HMA1 from *A.*

thaliana. Lastly, subgroups 1B-5 and 1B-6 include the remainder of the proteins in the P_{IB}-ATPase family that could not be included in any of the mentioned groups. Their ion specificity have yet to be discovered (1).

Table 1: Structural characteristics of each subgroup in the P_{IB}-ATPase subfamily. Metal specificity for each protein subgroup is shown in addition to the signature conserved sequences in transmembrane regions H6-H8 and N-MBD.

Subgroup	Metal specificity	N-MBD	H6	H7	H8
1B-1	Cu ⁺ /Ag ⁺	0-6 CXXC	CPC	NX ₆ YNX ₄ P	MX ₂ SSX ₅ [N/S]
1B-2	Zn ²⁺ /Cd ²⁺ /Pb ²⁺	0-2 CXXC + (HX) _n	CPC	NX ₇ K	DXGX ₇ N
1B-3	Cu ²⁺ /Cu ⁺ /Ag ⁺	H-rich	CPH	NX ₅ GYNX ₄ P	PXMSXSTX ₅ N
1B-4	Co ²⁺	-	SPC (H4)	not-identified	HEG[G/S]TX S[N/S][G/A/S]
1B-5	?	-	TPC	not-identified	not-identified
1B-6	?	?	?	not-identified	not-identified

As previously mentioned, P_{IB}-ATPases typically contain eight transmembrane fragments and a characteristic cytoplasmic loop between the sixth and seventh transmembrane fragments. This loop in the protein is the site of ATP-binding and phosphorylation of an important Asp residue in the sequence DKTGT (2,5). In the sixth transmembrane fragment, there are common signature sequences that are involved in metal binding: CPC, CPH, CPS, SPC, and TPC (1,6,10). These amino acid residues are critical for enzyme function. Experiments have shown that when the Cys residues are mutated in CopA from *A. fulgidus*, enzyme activity is lost. This short motif lies closely upstream from the phosphorylation domain (Figure 2). In addition, some P_{IB}-ATPases

have a common N-MBD in the cytoplasm with a CxxC motif. The Wilson and Menkes disease proteins contain six CxxC sequences in the N terminus, yet copper binds with a stoichiometry of only one copper atom per metal-binding repeat (12). Other proteins containing these N-MBDs include CadA from *Listeria monocytogenes*, which transports Cd^{2+} (8) and the Zn^{2+} transporter ZntA from *E. coli*, which also contain a CxxC motif (23). Other proteins contain His rich N-MBD, including *E. hirae* CopB (9) and CopB from *A. fulgidus* (11).

Originally, the N-terminal metal binding domain was believed to be required in metal binding and transport. The role of the metal binding domain was further explored, and it was shown that it is not required for enzymatic activity. After removal of this domain or causing a point mutation in the Cys of the CxxC consensus sequence, protein activity was not completely abolished. Therefore, this domain was proposed to have a regulatory role in the enzyme (8,10,11,26,27).

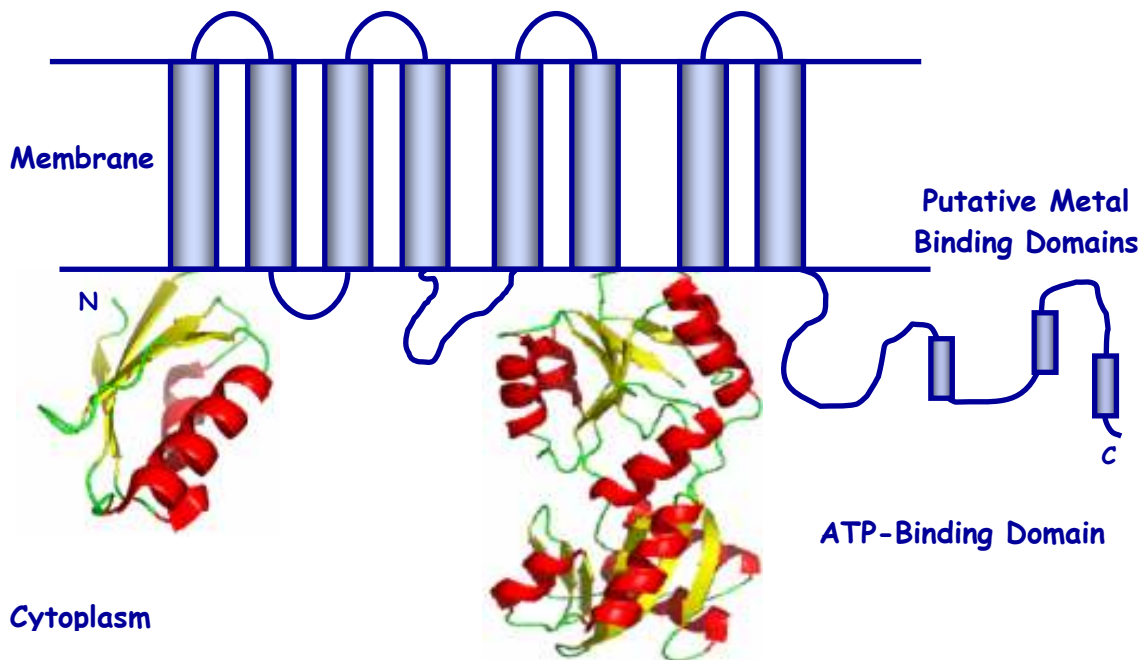


Figure 2: General Topology of $\text{P}_{1\text{B}}$ -ATPase
(Courtesy of Elif Eren)

1.3 Metal -Transport Mechanism

The transport mechanism of P_{1B}-type ATPases can be characterized by the catalytic cycle similar to all P-type ATPases. Conformational changes in the proteins occur within two states: E₁ and E₂ (3,29,30). As mentioned, this mechanism is characterized by the coupled ion translocation and ATP hydrolysis (30). The transport process is made up of a series of steps: ion binding, conformational changes in the protein, and ion release to the extracellular domain. Metals bind to a high-affinity site in the ATPase E₁ state, which triggers the phosphorylation of the conserved Asp residue in the DKTGT sequence of the enzyme by Mg²⁺-ATP. The change to the phosphorylated intermediate causes the protein to switch to the E₂ conformation. This step occurs with a reduced affinity for ions, which allows the translocation of metals to the other side of the membrane. Finally the phosphate group is released and the protein restores its original state (Figure 3) (29,30,31).

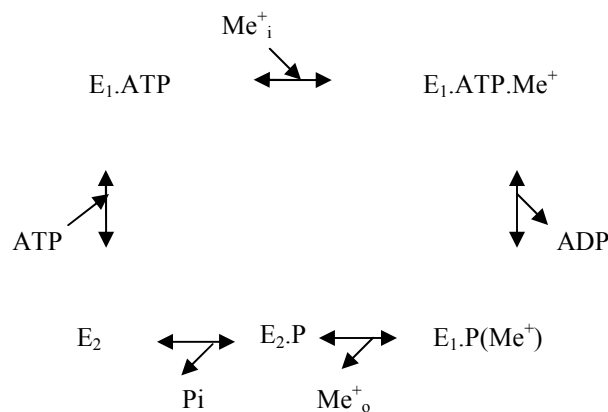


Figure 3: Scheme of P_{1B}-ATPase catalytic cycle. E₁ and E₂ are conformational states of the enzyme. Me⁺ is the metal ion being transported. Subscripts i and o corresponds to intracellular and outside of the cell, respectively. (Courtesy of Elif Eren)

1.4 Lipids and Membrane Protein Stability

Complex membrane proteins such as P_{IB}-ATPases are abundant in many types of organisms and found in various environments corresponding to where the organism thrives (2). These proteins must maintain structural qualities in order to function properly. Protein stability is influenced by a number of factors beginning with the amino acid sequence. This primary protein structure underlies the interactions in which a protein can form traditional α -helices and β -sheets in the secondary structure, and further onto the tertiary and quaternary structures. Electrostatic forces and H-bonding also contribute to proper protein folding and stability (33).

An important factor regarding protein folding and stability does not solely lie within the amino acid sequences, but the surrounding environments. Heat-thriving organisms have similar protein structures compared with those of mesophilic proteins. However under extreme temperatures, ordinary mesophilic membrane proteins would denature completely and lose all enzymatic function. Thermophilic membrane proteins are far more stable than the mesophilic counterparts and utilize higher temperatures for enzymatic activity (34).

Lipid bilayers surround membrane proteins. Composed of non-polar chains with various head groups, lipids are essential for membrane proteins to maintain enzymatic activity (35). The structures of lipids in the bilayer ultimately affect the fluidity of the membrane, resulting in either a stable arrangement suitable for high temperatures (decreased fluidity) or a delicate array of short rigid lipids observed in psychrophiles (increased fluidity) (34). Some characteristics that correlate with an increase in membrane fluidity are unsaturation, cis double bonds, chain shortening, methyl

branching, or cys-unsaturation. The proteins within these fluid membranes are directly affected by the lipid arrangements, corresponding to decreased stability (34,35). Typically, mesophiles and psychrophiles contain more fluid membranes, composed of lipids such as diphosphatidylglycerol and other glycerophospholipids. Archaea and other thermophiles contain ether-linked lipids that may be twice the normal glycerol chain length. In some cases the lipids form cyclic tetraethers by attaching to a second glycerol backbone (35). In this case, they expand the whole membrane thickness. This is one possible system for enhancing thermophilic protein stability.

1.5 Project Overview

This study was done with the goal of providing a set of molecular tools for thermostability analysis on Zn^{2+} transporting ATPases. P_{1B}-ATPase gene sequences were analyzed and proteins from three organisms were selected based on sequence identity and environmental growth conditions. *Pyrococcus abyssi* (thermophilic), *Escherichia coli* (mesophilic), and *Exiguobacterium 255-15* (psychrophilic) contain Zn-ATPases in their genomic sequences. The first goal of this work was to clone each one of these Zn-ATPase genes and express the proteins in *E. coli* cells. Once the proteins were expressed, each protein was purified from membranes and tested for ATPase activity to check if it was functional.

The second half of this project focuses on archaea growth and lipid extractions. As mentioned earlier, lipids are critical for protein stability. *Thermotoga maritima* and *Archaeoglobus fulgidus* are sulfide-reducing anaerobes that contain P-type ATPases. These archaea were grown and harvested. Cell membrane lipids were extracted from

each archaea, in parallel with *E. coli* lipids. With the availability of thermophilic lipids and a unique set of Zn^{2+} -ATPase constructs, future physicochemical studies will be able to provide valuable information on protein stability and enzymatic activity. The ultimate goal could pertain to incorporating thermophilic tetraether lipids with P-type ATPases from mesophilic or psychrophilic organisms.

2.0 Materials and methods

2.1 Cloning and Protein Expression

Genomic DNA from *E. Coli*, *P. abyssi*, and *Exiguobacterium 255-15* was used to isolate the gene coding for homologous Zn-ATPases. PCR was used to amplify these genes using primers that sit on the 5' and 3' ends of the predicted sequences (Table 1). Annealing temperature was set at 50°C for 1 min and elongation temperature was set at 72°C for 3 min. QuickStart (Qiagen), a proofreading polymerase was used to ensure a low error rate in the coding sequence for the amplification process. Agarose DNA purification allowed for the isolation of the genes of interest.

Two cloning vectors were used: pBAD TOPO/His and pCRT7/NT-TOPO/His (Invitrogen, Carlsbad, CA). Each PCR product containing the DNA sequence for the Zn-ATPases of the respective organism was ligated into the cloning sites of the vectors and transformed into Top10F' and LMG194 *E. coli* competent cells. Cells were heat shocked for 1 minute at 42°C and grown in 2XYT media for 1 hour at 37°C. Ampicillin (100 mg/mL) 2XYT plates were used for overnight growth at 37°C, and colonies were picked and screened by PCR and restriction digest for proper insert orientation.

LMG194 and Top10F' cells were grown until $OD_{600} = 0.6$. For samples containing pBAD TOPO/His vector, 0.02% L-arabinose was added to induce protein expression. Samples containing pCRT7/NT-TOPO/His vector were induced with 1mM isopropyl β -D-thiogalactopyranoside (IPTG). After the inducers were added, cells were grown for an additional 4 hours at 37°C.

Individually induced samples were run on 10% SDS-PAGE (Laemmli 1970) gels and stained with coomassie blue to observe protein presence. SDS-PAGE gels were transferred to nitrocellulose (NC) membranes at 350 mA for 90 minutes at 4°C. NC membranes were blocked with Buffer 229 (50mM Tris pH 7.4, 0.2M NaCl) and 5% milk for 30 minutes. Rabbit polyclonal IgG Anti-6X-His primary antibody (1:2000)(Affinity bioreagents, Golden, CO), Buffer 229, and 5% milk were incubated with the NC membranes overnight at 4°C with gentle rocking. NC membranes were washed three times for 5 min with Buffer 229, 5% milk, and 0.05% Tween-20. Donkey Anti-Rabbit IgG secondary antibody (1:1000)(Affinity bioreagents, Golden, CO), Buffer 229, and 5% milk were incubated with the transfer membranes at room temperature for 1-2 h. Again, the NC membranes were washed three times with Buffer 229, 5% milk, and 0.05% Tween-20. Supersignal® West Pico Chemiluminescent reagents were added to the NC membranes, films were exposed and developed to observe protein expression.

2.2 Protein Purification

Membrane purification was carried out as previously described (6). Cells were suspended in buffer A (25 mM Tris pH 7.0, 100 mM sucrose, 1 mM phenyl methyl sulfonyl fluoride (PMSF)) and homogenized 6 times at 30 sec intervals using a BeadBeater (BioSpec Products, Bartlesville, OK). After addition of 0.02 mg/ml Danes I and 2 mM MgCl₂, the homogenate was incubated for 30 min at 4°C. Lysed cells were centrifuged at 8,000 x g for 30 min. The supernatant was then centrifuged at 163,000 x g for 1 h. Membranes were resuspended in buffer A (5-15 mg/ml) and stored at -80°C.

For protein solubilization, membranes were diluted to 3 mg/mL with buffer B (25 mM Tris-Cl pH 8.0, 100 mM sucrose, 500 mM NaCl, 1 mM PMSF). Triton X-100 was added to a final concentration of 1%, and the membrane preparation was incubated with the detergent for 1 h at 4°C with gentle stirring. The suspension was cleared by centrifugation at 229,000 x g for 1 h and Ni²⁺-nitrilotriacetic acid (Ni-NTA) resin (Quiagen, Valencia, CA) pre-equilibrated with buffer B plus 0.5% Triton X-100 and 5 mM imidazole was added to the supernatant.

After 1 h, the Ni²⁺ resin and solubilized protein were both loaded back into the columns and washed with buffer B and 5 mM imidazole, and then buffer B with 20 mM imidazole. The protein was eluted with buffer B and 300 mM imidazole. Fractions were collected for the elution, and an SDS-PAGE gel was run to observe which fractions contained the protein. The fractions containing the protein were concentrated by filtration in 50,000 MW centricon (Millipore, Billerica, MA) and imidazole was removed using a Sephadex G-25 column. The protein was eluted with buffer C (25 mM Tris-Cl pH 8.0, 100 mM sucrose, 50mM NaCl, 1 mM PMSF, 1 mM DTT, and 0.5% Triton X-100). All protein determinations were performed in accordance with Bradford (17).

2.3 ATPase Activity Assays

ATPase activity assays were carried out as previously described (6). ATPase activity assay mixture contained 50 mM Tris pH 6.1, 3 mM MgCl₂, 3 mM ATP, 20 mM Cys, 0.01% asolectin, 0.02% Triton X-100, 800 mM NaCl, 10 µg purified enzyme, and 100 µM or 500 µM ZnSO₄. Released inorganic phosphate (Pi) was determined in

accordance to Lanzetta et al (32). ATPase activity was measured for 10 min at 37°C, 75°C, and room temperature.

2.4 *Thermotoga maritima* growth

One liter of mineral mix (4x) was prepared containing 1 g NH₄Cl, 0.2 g CaCl₂, 0.2 g K₂HPO₄, 20 g KCl, and 13.8 g MgSO₄. *Thermotoga maritima* media containing 500 mL mineral mix (4x), 500 mL ddH₂O, 4.8 g HEPES, 20 g NaCl, 10 mL vitamin mix (ATCC #: MD-VS), 0.5 g cysteine, and 5 g yeast extract was dissolved at room temperature. Next, 0.5 g cystine was added to 6.6 mL 1M NaOH. This was added to the media mix and pH was adjusted to 7.4-7.5. Media was distributed in glass bottles and autoclaved (uncovered) for 30 min to remove dissolved oxygen. For anaerobic media, the glass bottles were covered with stopper/septum and N₂ gas was run through the media for 30 min. Next a vacuum was applied, and the head space was also gassed with N₂ for 15 min. Cells were inoculated (1%) in the new media and grown overnight at 77°C.

2.5 *Archaeoglobus fulgidus* growth

One liter of salt solution (10x) was prepared containing 34.5 g MgSO₄, 3.4 g KCl, 27.5 g MgCl₂, 2.5 g NH₄Cl, and 180 g NaCl. A set of trace element solutions (1000x) were also prepared separately. These 100 mL solutions contained 18.0 g K₂HPO₄, 14.0 g CaCl₂, 0.20 g Fe(NH₄)₂(SO₄)₂, and 0.038 g Na₂WO₄. A one liter mineral stock (100x) was prepared containing 2.74 g Na₂EDTA, 6.14 g MgSO₄, 0.5 g MnSO₄, 1.0 g NaCl, 0.18 g FeSO₄, 0.13 g CaCl₂, 0.18 g ZnSO₄, 0.22 g CoCl₂, 0.018 g AlK(SO₄)₂, 0.016 g CuSO₄, 0.012 g Na₂MoO₄, and 0.010 g H₃BO₃. For preparing the media, 650 mL dH₂O and 100 mL 10x salt solution was combined. Next, 1.0 mL of each trace element

solution was added to the mix. This was followed by adding 10 mL mineral stock (10x) and 10 mL vitamin mix (ATCC #: MD-VS). As a carbon source, 7.6 g Pipes sodium salt was added in addition to 1.5 g sodium lactate. The pH was adjusted to 7.0 with 10 M NaOH and the volume was topped off with dH₂O to just over one liter (to accommodate evaporation). The media was boiled on a hot plate for 10 min while sparging with nitrogen gas. Sparging was continued for the entire cooling process as well. The media was dispersed to smaller glass containers, and the head space was gassed with nitrogen as well. The bottles were sealed and autoclaved.

Before inoculating the new media, 0.5 M anaerobic sodium sulfide was added to the media as a reducing agent. The media was inoculated (1%) with *A. fulgidus* cells (ATCC: 49558) and grown for two days at 83°C.

2.6 Lipid extraction and Thin Layer Chromatography

Membrane lipids were extracted similar to the previously described (33). 500 mg cells were resuspended in 19 mL chloroform: methanol: 5% TCA (1:2:0.8) and stirred for 2-3 h. The contents were transferred to a separatory funnel, and 5 mL chloroform was added. After mixing well, 5 mL water was also added to the funnel. The separatory funnel was left to sit at 4°C overnight to allow complete phase separation. The lower phase (chloroform phase) was collected and washed 2X with 1.9 volumes of methanol: water (1:0.8). Lipids were diluted by 10% with benzene and evaporated to dryness with a rotary evaporator. Lipids were redissolved in minimal chloroform: methanol (1:1). Silica plates were used for thin layer chromatography (TLC). Running solvents for TLC

contained chloroform:methanol:water (65:25:10) or hexane:ethyl acetate:acetic acid (80:20:1). Plates were developed with iodine vapor.

3.0 Results

3.1 *Escherichia coli*, *Pyrococcus abyssi*, and *Exiguobacterium 255-15*: Sequence homology

The organisms of interest in this study contain Zn²⁺ transporting ATPases. The DNA sequences for these proteins were obtained using GenBank (www.ncbi.com). Their sequences contain the signature amino acid residues for the coordination and binding of Zn²⁺. Each protein contains the site of phosphorylation, DKTGT, resulting from ATP hydrolysis. More notably these proteins belong to the IB-2 group, which all contain the consensus sequence NX(7)KX(10,20)DXGX(7)N within H7 and H8 (Figure 4)(1).

	<u>H6</u>	
E. coli:	KGLTLLIF C PCALVI S TFAAITSGLAAAARRGALIKGGAALEQLGRVTQVAF D KTGT	440
P. abyssi:	RALVILVIS C PCALVLSIPLGYFGGIGRAAKEGILIKGSNYLDALKDASIVAF D KTGT	397
Exiguobacterium:	RALVFLVIS C PCALVI S IPLGFFSGIGAASKRGILVKGGNHLEALQQLDVTVF D KTGT	416
	<u>H7</u>	<u>H8</u>
E. coli:	RQNIITIALGL K GIELVTLL G MTGLWLAVLA D TGATVLVTA N ALRLLRRR	732
P. abyssi:	WENIIFALGV K LAFIPLGIF G KATMWEAVFA D VGVVALIAVF N AMRVLR	689
Exiguobacterium:	YQNIAFALGI K GVFLLGAF G VATMWEAVFA D VGVTVLAVL N AMRILR	708

Figure 4: Sequence alignments of each Zn-ATPase. IB-2 conserved amino acids are colored in red. The numbers correspond to amino acid position in the protein.

3.2 Cloning of Zn-ATPases into pBAD TOPO and pCRT7/NT

Genomic DNA from *E. coli*, *P. abyssi*, and *Exiguobacterium 255-15* was used to isolate the genes coding for Zn²⁺ transporting ATPases. Primers in the 5' and 3' directions sitting at each end of the genes were designed for PCR amplification (Sigma-Aldrich) (Appendix A). The expected band sizes for *E. coli*, *P. abyssi*, and *Exiguobacterium 255-15* were 2.2 kb, 2.0 kb, and 2.1 kb, respectively. A clear band was obtained under ultraviolet light for each cDNA run in a 1% agarose gel, and the primers showed no contamination (Figure 5).

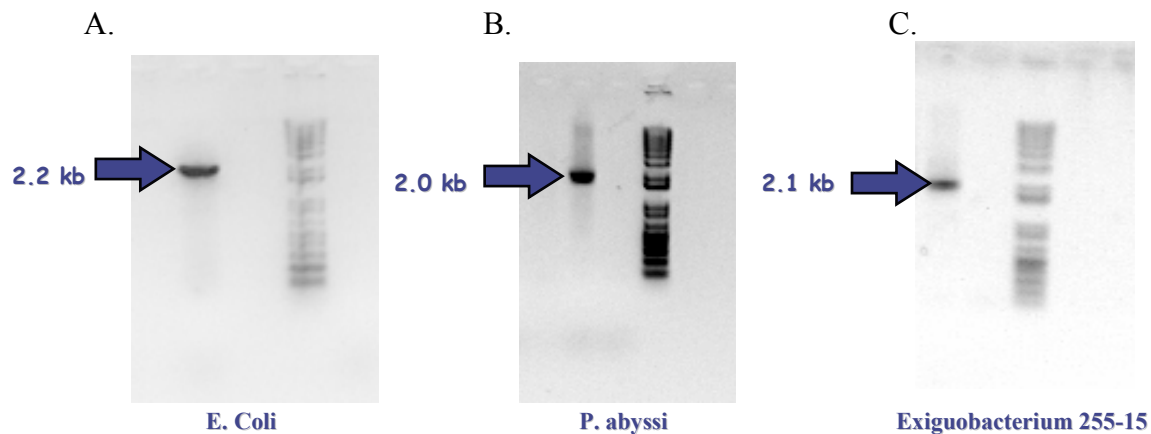


Figure 5: PCR amplification of *E. coli*, *P. abyssi*, and *Exiguobacterium 255-15* Zn-ATPases. *A.* Lane 1: *E. coli* genomic DNA. Lane 2: Neg ctrl (No DNA). Lane 3: 1 kb ladder. *B.* Lane 1: *P. abyssi* genomic DNA. Lane 2: Neg ctrl (No DNA). Lane 3: 1 kb ladder. *C.* Lane 1: *Exiguobacterium 255-15* genomic DNA. Lane 2: Neg ctrl (No DNA). Lane 3: 1 kb ladder.

Upon completion of the initial PCR, the DNA was extracted from the gel and ligated into pBAD TOPO and pCRT7/NT for *E. coli*, *P. abyssi*, and *Exiguobacterium 255-15*. Multiple competent cells were transformed in different combinations with the DNA plasmids to eventually create many strains that were used to test for expression of these proteins (Table 2). Top10F⁷ cells tended to produce colonies consistently in both vectors, so they were screened by PCR (Figure 6). The primers used here were a bit different than the previous PCR but the expected band sizes were very similar. Only one of the primers has to sit on the end of the gene in either the 5' or 3' direction. The complementary primer must amplify a portion of the vector, again in either the 5' or 3'

direction (Appendix A). The purpose of this screening is to identify whether or not the gene insert (Zn-ATPase) is in the correct orientation in the vector.

Table 2: Clone constructs created

Organism	Expression Vector	Transformed Cell Lines
<i>E. coli</i>	pBAD TOPO	Top10F', LMG194, BL21star(DE3), BL21AI
<i>P. abyssi</i>	pBAD TOPO	Top10F', Top10, LMG194
<i>Exiguobacterium 255-15</i>	pBAD TOPO	Top10F'
<i>E. coli</i>	pCRT7/NT	BL21AI, BL21(DE3), BL21star(DE3), BL21star(DE3)pLysS
<i>P. abyssi</i>	pCRT7/NT	Top10F'
<i>Exiguobacterium 255-15</i>	pCRT7/NT	Top10F'

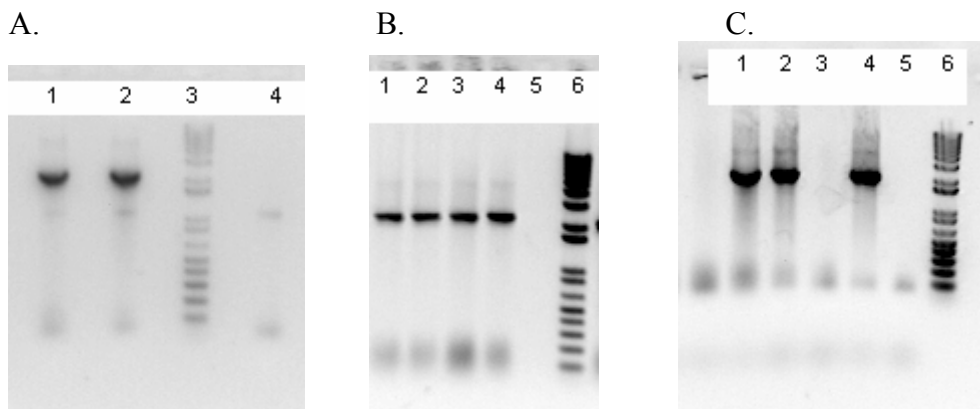


Figure 6: PCR screening for insert orientation in *E. coli*, *P. abyssi*, and *Exiguobacterium 255-15* Zn-ATPases. Top10F' competent cells were used in each gel. **A.** Lanes 1 + 2: Positive colonies with *E. coli* - pBAD TOPO vector. Lane 3: 1 kb ladder. Lane 4: Neg ctrl (no DNA) **B.** Lanes 1-4: Positive colonies for *P. abyssi* - pBAD TOPO. Lane 5: Neg ctrl (no DNA). Lane 6: 1 kb ladder. **C.** Lanes 1, 2, and 4: Positive colonies for *Exiguobacterium 255-15* - pCRT7/NT. Lane 3: Negative colony. Lane 5: Neg ctrl (no DNA). Lane 6: 1 kb ladder

As a method to double check orientation, restriction digests for selected positive colonies were carried out (Figure 7). For *E. coli*-pBADTOPO construct, HincII was used to obtain two fragments: 4782 bp and 1538 bp. BsaB1 was used for *P. abyssi*-

pBADTOPO construct, yielding two fragments: 3495 bp and 2696 bp. Finally, *Exiguobacterium*-pCRT7nt construct was cut with PciI, yielding two DNA fragments: 3067 bp and 1921 bp. These digests confirmed the correct orientation of the Zn-ATPase inserts.

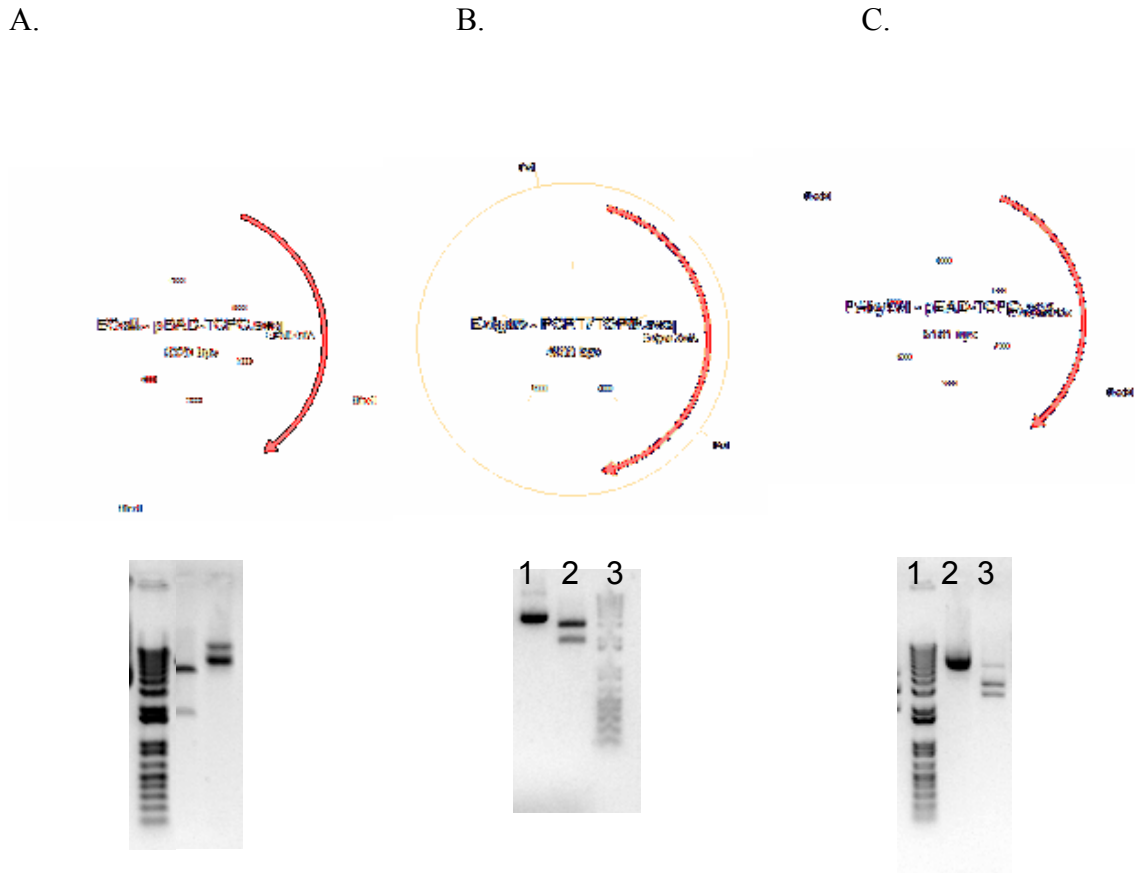


Figure 7: Cloning maps and restriction digests. **A. Upper.** Cloning map of *E. coli*-pBADTOPO construct. Red arrow indicates gene insert. **Lower.** Lane 1: 1 kb ladder. Lane 2: HincII cut DNA. Lane 3: Uncut DNA. **B. Upper.** Cloning map of *Exiguobacterium*-pCRT7nt construct. Red arrow indicates gene insert. **Lower.** Lane 1: Uncut DNA. Lane 2: PciI cut DNA. Lane 3: 1 kb ladder. **C. Upper.** Cloning map of *P. abyssi*-pBADTOPO construct. Red arrow indicates gene insert. **Lower.** Lane 1: 1 kb ladder. Lane 2: Uncut DNA. Lane 3: BsaB1 cut DNA

3.3 Expression of *E. coli*, *P. abyssi*, and *Exiguobacterium 255-15* Zn-ATPases

After the clones were confirmed to contain the insert in the correct orientation, the Top10F' cells were grown with chemical inducers to test for protein expression. For

each enzyme being studied, protein expression was attempted many times using the various strains shown in Table 2. Some of these could not express. The proteins from some of the samples expressed once and could not be repeated. However, the Top10F' clones expressed these proteins most consistently. For Top10F' stocks containing pBAD TOPO, L-arabinose was used to induce as mentioned in the methods section. Similarly, stocks containing pCRT7/NT were induced with IPTG. Western analysis of the samples clearly shows Zn-ATPase expression in *E. coli*, *P. abyssi*, and *Exiguobacterium 255-15* (Figure 8).

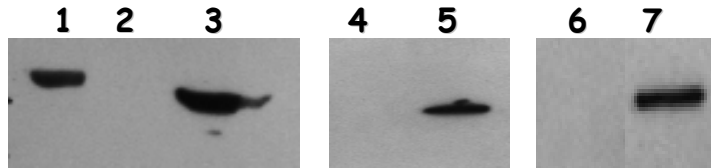


Figure 8: Expression of *E. coli*, *P. abyssi*, and *Exiguobacterium 255-15* Zn-ATPases using His₆-tagged expression vectors. Lane 1: CopA (Pos ctrl) Lane 2: *E. coli* uninduced Lane 3: *E. coli* induced Lane 4: *P. abyssi* uninduced Lane 5: *P. abyssi* induced Lane 6: *Exiguobacterium* uninduced Lane 7: *Exiguobacterium* induced

3.4 Purification of *E. coli*, *P. abyssi*, and *Exiguobacterium 255-15* Zn-ATPases

Membrane samples were collected for each organism. Each membrane preparation yielded 15-23 mg protein for one liter of cells (Table 3). Some of the protein was lost during the initial homogenization, but enough protein was present to move on to the purification procedure.

Purification for each Zn-ATPase was done simultaneously at 4°C to prevent proteases from degrading the enzyme. The membrane preparations yielded below average quantities of protein, so the Ni-NTA slurry was fixed at 0.8 mL. *E. coli*, *P. abyssi*, and *Exiguobacterium 255-15* all followed the exact same protocol with no

specific alterations. Aliquots of 1 mL were collected for each wash in order to monitor where the purified protein was in the column. Protein gels were run with selected aliquots to observe the final purified protein before passing through the Sephadex-G25 column. Again, purified protein yields were very low (Table 3). In most cases, the purified Zn-ATPase was eluted rather quickly after the addition of 300 mM imidazole. Figure 9 illustrates *E. coli*, *P. abyssi*, and *Exiguobacterium 255-15* purified proteins and a comparison with membrane samples.

Table 3: Purification Yields

Organism	Mem Prep mg/ml	Vol ml	Tot membr prot mg	Membr/cell mg/g
E. Coli #1	10.40	1.50	15.60	2.97
E. Coli #2	7.75	2.50	19.38	3.66
E. Coli #3	5.43	3.00	16.29	4.36
P. abyssi #1	7.18	2.50	17.95	6.41
P. abyssi #2	5.65	3.00	16.95	6.25
Exiguobacterium	5.56	4.00	22.24	4.73
	Purified protein mg/ml	Vol mL	Total protein mg	Prot/Membr mg/mg
E. Coli #1	0.11	1.00	0.11	0.0071
E. Coli #2	1.17	1.00	1.17	0.0604
E. Coli #3	0.77	1.50	1.16	0.0709
P. abyssi #1	0.42	1.00	0.42	0.0234
P. abyssi #2	0.57	1.50	0.86	0.0504
Exiguobacterium	0.48	2.00	0.96	0.0432

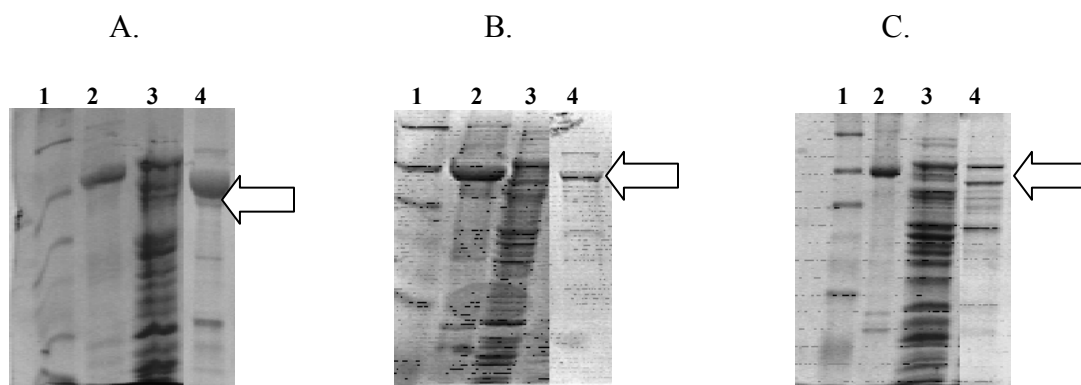


Figure 9: Purification of *E. Coli*, *P. abyssi*, and *Exiguobacterium 255-15* Zn-ATPases. **A. *E. coli*** Lane 1: Protein marker. Lane 2: Pos ctrl (CopA). Lane 3: *E. coli* membrane prep. Lane 4: Purified *E. coli* Zn-ATPase indicated with arrow. **B. *P. abyssi*** Lane 1: Protein marker. Lane 2: Pos ctrl (CopA). Lane 3: *P. abyssi* membrane prep. Lane 4: Purified *P. abyssi* Zn-ATPase indicated with arrow. **C. *Exiguobacterium 255-15*** Lane 1: Protein marker. Lane 2: Pos ctrl (CopA) Lane 3: *Exiguobacterium 255-15* membrane prep. Lane 4: Purified *Exiguobacterium 255-15* Zn-ATPase indicated with arrow.

3.5 ATPase activity

Activity assays were attempted several times for each organism. *P. abyssi* showed ATPase activity with two different samples, but with a low activity of 2.75 $\mu\text{mol}/\text{mg}/\text{hr}$. The only other activity that was observed was from a membrane preparation of *E. coli* cells, 1.33 $\mu\text{mol}/\text{mg}/\text{hr}$. Table 4 shows the quantified activity of the proteins. *E. coli* Zn-ATPase activity was observed at a much higher level in previous work (32). ATPase activity for *Exiguobacterium 255-15* was also attempted at room temperature and 10°C, but no activity was observed.

Table 4: ATPase Activity Yields

Sample	Activity
	umol/mg/hr
E. coli #2 (mem)	1.33
P. abyssi #1	2.74
P. abyssi #2	2.75
Mitra E. coli	14.82

3.6 Archaea Growth and TLC analysis

Both archaea of interest, *T. maritima* and *A. fulgidus*, were grown successfully under anaerobic conditions. The major difference in growing the two organisms was the method of sulfide reduction. *T. maritima* uses cysteine as a reducing agent, while *A. fulgidus* requires a stronger substance like sodium sulfide. In fact, sodium sulfide came to be the biggest problem in growing *A. fulgidus*. Sodium sulfide is extremely basic, so it would make sense to neutralize the pH before adding it to neutral media. However, preparing a neutral stock of this proved to be extremely difficult and time consuming. The way around this problem was simply adding a non-neutralized stock to the media in small amounts.

Unlike *E. coli* cells that produce nearly 4.5 g cells/liter, these sulfide reducing archaea grow at a much lower confluence. One liter of *T. maritima* media yielded 0.96 g cells. Similarly, one liter of *A. fulgidus* media yielded 0.59 g cells. Although the quantity of cells was low, it was enough to extract lipids for TLC analysis.

TLC was run several times in order to observe visible lipid bands. The first running solvent that was used contained chloroform:methanol:water (65:25:10). The lipids appeared as a single glob or nothing at all when developed under iodine vapor.

The running solvent was then switched to hexane:ethyl acetate:acetic acid (80:20:1). This solvent worked much better in producing visible bands. Figure 10 shows the difference in running solvents, and the presence of lipids in each extract. One concern is for the phospholipid standard that was used, which no band appeared. However, it is clear that lipids are present in all samples, and the thermophilic archaea contain different lipids than the mesophilic *E. coli* lipids, as expected.

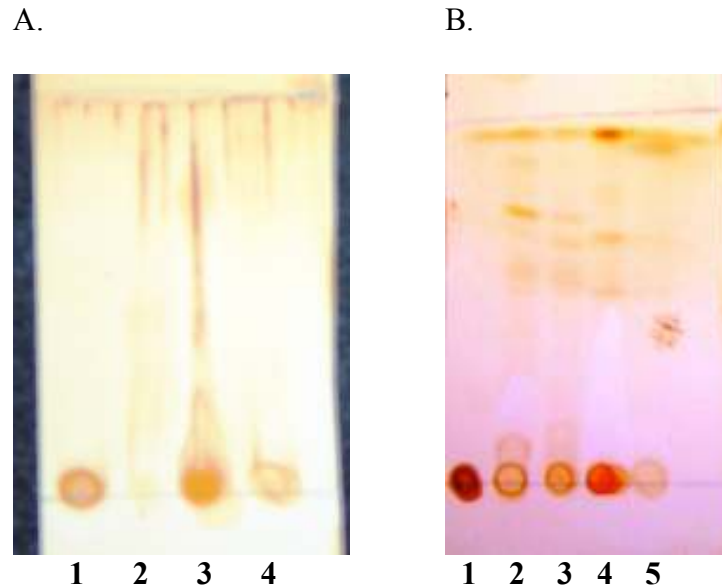


Figure 10: TLC plates of lipid extracts from *E. coli*, *Thermotoga maritima*, and *Archaeoglobus fulgidus*. **A. Chloroform:Methanol:Water solvent** Lane 1: Phospholipid standard. Lane 2: *E. coli* lipids. Lane 3: *T. maritima* lipids. Lane 4: *A. fulgidus* lipids. **B. Hexane:Ethyl acetate:Acetic acid solvent.** Lane 1: Phospholipid standard. Lane 2: *E. coli* lipids #1. Lane 3: *E. coli* lipids #2. Lane 4: *T. maritima* lipids. Lane 5: *A. fulgidus* lipids

4.0 Discussion

E. coli, *P. abyssi*, and *Exiguobacterium 255-15* are model organisms containing Zn-ATPases. With each organism thriving at unique temperatures, it sets up this work for further studies on protein stability. It is hypothesized that thermophilic organisms contain stable proteins because they can withstand such high temperatures without degrading. The tools from this project allow future work to be accomplished regarding protein stability and lipid surroundings

The cloning constructs will provide many possible sources of transformed cells in various expression vectors. Although many cloning constructs were created, there were three main constructs which were the focus of this project: *E. Coli*-pBADTOPO, *P. abyssi*-pBADTOPO, and *Exiguobacterium 255-15*-pCRT7/NT. These Zn-ATPase proteins were expressed successfully after adding a chemical inducer. The DNA sequences were also confirmed to be correct. This implies that there was no random mutation during the cloning process, and the protein should be folding and functioning normally.

Although it is expected that ATPase activity should be observed easily if the protein is expressing normally, it is not the case. Unfortunately there are several steps where protein activity can be lost. One example is during membrane preparation, where PMSF is used as a protease inhibitor. PMSF is known to be very short-lived and unstable. Perhaps adding additional protease inhibitors will increase the chance at observing protein activity, such as leupeptin and aprotinin. Another way to lose protein activity could simply come from contaminated buffers or water, which may also contain proteases. For this project, the yields obtained for membrane preparation and purification

were low. This could be another reason for a small amount of ATPase activity. The ATPase activity observed for the purified *P. abyssi* Zn-ATPase protein appeared low, but was duplicated with a separate sample. It raises a suspicion that perhaps there could be something reacting to give a false positive.

T. maritima and *A. fulgidus* were grown because they also contain heavy metal transporting ATPases and are found in thermophilic environments. All of the other constructs were transformed into mesophilic *E. coli* cells, so there was a need for living thermophilic cells. The lipids from these cells were extracted with the aim of incorporating the thermophilic lipids with the mesophilic and psychrophilic proteins. These lipids could potentially make the *E. coli* and *Exiguobacterium 255-15* Zn-ATPase proteins much more active at higher temperatures. This would be due to rapid ATP hydrolysis and structurally stronger lipids. Therefore, at higher temperatures the protein would remain intact. The purification that was done on *E. coli*, *P. abyssi*, and *Exiguobacterium 255-15* Zn-ATPases will allow for this type of analysis to take place. This could provide a whole new insight on altering lipid environments to avoid protein denaturation. A protein which may be difficult to study because of its endogenous environment could potentially be worked with much easier.

5.0 References

1. **Argüello JM** (2003) Identification of ion selectivity determinants in heavy metal transport P_{1B}-type ATPases. *J Membr Biol*, **195**: pp. 93–108
2. **Axelsen KB, Palmgren MG** (2001) Inventory of the superfamily of P-type ion pumps in Arabidopsis. *Plant Physiol* **126**: 696–706
3. **Axelsen KB, Palmgren MG** (1998) Evolution of substrate specificities in the P-type ATPase superfamily. *J Mol Evol* **46**: 84–101
4. **Eren E, Argüello JM** (2004) Arabidopsis HMA2, a Divalent Heavy Metal-Transporting P_{1B}-Type ATPase, Is Involved in Cytoplasmic Zn²⁺ Homeostasis. *Plant Physiology*, **136**: pp. 3712-3723
5. **Hall JL** (2002) Cellular mechanisms for heavy metal detoxification and tolerance. *J Exp Bot* **53**: 1–11
6. **Mandal AK, Cheung WD, Argüello JM** (2002) Characterization of a thermophilic P-type Ag⁺/Cu⁺-ATPase from the extremophile *Archaeoglobus fulgidus*. *J Biol Chem* **277**: 7201–7208
7. **Mills RF, Francini A, Aylett M, Krijger GC, Williams L** (2004) The plant P_{1B}-type ATPase AtHMA4 transports Zn and Cd and plays a role in detoxification of transition metals supplied at elevated levels. *FEBS Letters* **579**: 783-791
8. **Mitra, B., Sharma, R.** (2001) The cysteine-rich amino-terminal domain of ZntA, a Pb(II)/Zn(II)/Cd(II)-translocating ATPase from *Escherichia coli*, is not essential for its function. *Biochemistry* **40**:7694-7699
9. **Odermatt, A., Suter, H., Krapf, R., Solioz, M.** (1993) Primary structure of two P-type ATPases involved in copper homeostasis in *Enterococcus hirae*. *J Biol Chem* **268**:12775-12779
10. **Mandal AK., Arguello J.M.** (2003) Functional roles of metal binding domains of the *Archaeoglobus fulgidus* Cu(+)-ATPase CopA. *Biochemistry* **42**:11040-7
11. **Mana-Capelli, S., Mandal, A.K., Arguello, J.M.** (2003) *Archaeoglobus fulgidus* CopB Is a Thermophilic Cu²⁺-ATPase: functional role of its histidine-rich N-terminal metal binding domain. *J Biol Chem* **278**:40534-40541
12. **Lutsenko, S., Petris, MJ.** (2002) Function and regulation of the mammalian copper-transporting ATPases: Insights from biochemical and cell biological approaches. *J Membr Biol* **191**:1-12

- 13. Stadnitskaia, A., Omoregie, E., Boetius, A., Sinninghe Damsté, J.S.** (2006) Lipid composition and methanotrophic diversity in different fluid venting environments of the Nile deep-sea fan, Eastern Mediterranean. *Geophysical Research Abstracts* **8**: 04127
- 14. Oliver, James D., Stringer, William F.** (1984) Lipid Composition of a Psychrophilic Marine *Vibrio* sp. During Starvation-Induced Morphogenesis. *Appl Environ Microbiol* **47(3)**: 461–466.
- 15. Gounot, A. M., and N. J. Russell** (1999). Physiology of cold-adapted microorganisms In: R. Margesin and F. Schinner (Ed.) Cold-adapted Organisms: Ecology, Physiology, Enzymology and Molecular Biology. 33–55
- 16. Lutsenko, S., Petrukhin, K., Cooper, M.J., Gilliam, C.T., Kaplan, J.H.** 1997. N-terminal domains of human copper-transporting adenosine triphosphatases (the Wilson's and Menkes disease proteins) bind copper selectively *in vivo* and *in vitro* with stoichiometry of one copper per metal-binding repeat. *J Biol Chem* **272**:18939-18944
- 17. Bradford, M.M.** 1976. A rapid and sensitive method for the quantitation of microgram quantities of protein utilizing the principle of protein-dye binding. *Anal Biochem* **72**:248-254
- 18. Bull, P.C., Cox, D.W.** 1994. Wilson disease and Menkes disease: new handles on heavy-metal transport. *Trends Genet* **10**:246-52.
- 19. Bull, P.C., Thomas, G.R., Rommens, J.M., Forbes, J.R., Cox, D.W.** 1993. The Wilson disease gene is a putative copper transporting P-type ATPase similar to the Menkes gene [published erratum appears in *Nat Genet* 1994 Feb;6(2):214]. *Nat Genet* **5**:327-337
- 20. Paulsen, I.T., Saier, M.H., Jr.** 1997. A novel family of ubiquitous heavy metal ion transport proteins. *J Membr Biol* **156**:99-103
- 21. Petrukhin, K., Lutsenko, S., Chernov, I., Ross, B.M., Kaplan, J.H., Gilliam, T.C.** 1994. Characterization of the Wilson disease gene encoding a P-type copper transporting ATPase: genomic organization, alternative splicing, and structure/function predictions. *Hum Mol Genet* **3**:1647-56
- 22. Pufahl, R.A., Singer, C.P., Peariso, K.L., Lin, S.J., Schmidt, P.J., Fahrni, C.J., Culotta, V.C., PennerHahn, J.E., Ohalloran, T.V.** 1997. Metal ion chaperone function of the soluble Cu(I) receptor Atx1. *Science* **278**:853-856
- 23. Rensing, C., Mitra, B., Rosen, B.P.** 1997. The ZntA gene of *Escherichia coli* encodes a Zn(II)-translocating P-type ATPase. *Proc Natl Acad Sci U S A* **94**:14326-31
- 24. Rutherford, J.C., Cavet, J.S., Robinson, N.J.** 1999. Cobalt-dependent transcriptional switching by a dual-effector MerR-like protein regulates a cobalt-exporting variant CPx-type ATPase. *J Biol Chem* **274**:25827-25832

- 25. Sharma, R., Rensing, C., Rosen, B.P., Mitra, B.** 2000. The ATP hydrolytic activity of purified ZntA, a Pb(II)/Cd(II)/Zn(II)-translocating ATPase from *Escherichia coli*. *J Biol Chem* **275**:3873-3878
- 26. Voskoboinik, I., Mar, J., Strausak, D., Camakaris, J.** 2001. The regulation of catalytic activity of the menkes copper-translocating P-type ATPase. Role of high affinity copper-binding sites. *J Biol Chem* **276**:28620-7.
- 27. Voskoboinik, I., Strausak, D., Greenough, M., Brooks, H., Petris, M., Smith, S., Mercer, J.F., Camakaris, J.** 1999. Functional analysis of the N-terminal CXXC metal-binding motifs in the human Menkes copper-transporting P-type ATPase expressed in cultured mammalian cells. *J Biol Chem* **274**:22008-22012
- 28. Rensing, C., B. Fan, et al.** (2000). "CopA: An *Escherichia coli* Cu(I)-translocating P-type ATPase." *Proc. Natl. Acad. Sci. USA* **97**(2): 652-6.
- 29. Inesi, G.** (1985). "Mechanism of calcium transport." *Ann. Rev. Physiol.* **47**: 573-601.
- 30. Glynn, I. M.** (1985). The Na⁺,K⁺-transporting adenosine triphosphatase. *Enzymes of Biological Membranes*. A. Martonosi. New York, Plenum PL. **3**: 35-114.
- 31. Kuhlbrandt, W.** (2004). Biology, Structure and mechanism of P-type ATPases. *Nature Reviews Molecular Cell Biology*
- 32. Sharma, R., Rensing, C., Rosen, B., Mitra, B.** (2000) The ATP Hydrolytic Activity of Purified ZntA, a Pb(II)/Cd(II)/Zn(II)-translocating ATPase from *Escherichia coli*. *J. Biol. Chem*; **275**: 3873 - 3878
- 33. Toyoshima, C., and Nomura, H.** (2002) Structural changes in the calcium pump accompanying the dissociation of calcium. *Nature* **418**: 605-611
- 34. Lehtinen, P., KiiliaÈinen , K., LehtomaÈki, I., Laakso, S.** (2002). Effect of heat treatment on lipid stability in processed oats. *Journal of Cereal Science* **37**: 215-221
- 35. Walraven, H., Koppenaar, E., Marvin, H., Hagendoorn, M., Kraayenhof, R.** (1984) Lipid specificity for the reconstitution of well-coupled ATPase proteoliposomes and a new method for lipid isolation from photosynthetic membranes. *European Journal of Biochemistry* **144**: 563

Appendix: Primers used for PCR amplification and DNA sequencing

Primer Name	Recognition Sequence
pBAD Reverse	GATTTAATCTGTATCAGG
pBAD Forward	ATGCCATAGCATT TTTTATCC
pCRT7 Reverse	TAGTTATTGCTCAGCGGTGG
pCRT7 forward	TAATACGACTCACTATAGGG
5' E coli ZntA	TCGACTCCTGACAATCACGGC
3' E. coli ZntA	TCTCCTGCGCAACAATCTTAACG
5' P abyssi	ATGCCTCGGAAGCTTAAGTTAGAA
3' P abyssi	CCTTAAGACTCTCATCGCGTTA
5' Exiguo ZntA	ATGGAAGCGAAAACAGAACGT
3' Exiguo ZntA	TTTTCGTAAAATCCGCATCGC
5' Ecoli ZntA 2	GAAACCTTAATGAGCGTAGCC
3' Ecoli ZntA 2	AACGCAATGACACCAAGCACG
5' P abyssi 2	TATGGCTGTAGATAAGTCAAG
3' P abyssi 2	TTTTATTTTCATCAGATATCAC
5' Exiguo ZntA 2	GTCGCTGTCATGTTGTTTTAT
3' Exiguo ZntA 2	CCGGATAAATCCAAGGTAGCT

